

Asymmetric, Helical, and Mirror-Symmetric Traveling Waves in Pipe Flow

Chris C. T. Pringle* and Rich R. Kerswell†

Department of Mathematics, University of Bristol, University Walk, Bristol BS8 1TW, United Kingdom

(Received 20 March 2007; published 16 August 2007)

New families of three-dimensional nonlinear traveling waves are discovered in pipe flow. In contrast with known waves [H. Faisst and B. Eckhardt, *Phys. Rev. Lett.* **91**, 224502 (2003); H. Wedin and R. R. Kerswell, *J. Fluid Mech.* **508**, 333 (2004)], they possess no discrete rotational symmetry and exist at a significantly lower Reynolds numbers (Re). First to appear is a mirror-symmetric traveling wave which is born in a saddle node bifurcation at $Re = 773$. As Re increases, “asymmetric” modes arise through a symmetry-breaking bifurcation. These look to be a minimal coherent unit consisting of one slow streak sandwiched between two fast streaks located preferentially to one side of the pipe. Helical and nonhelical rotating waves are also found, emphasizing the richness of phase space even at these very low Reynolds numbers.

DOI: [10.1103/PhysRevLett.99.074502](https://doi.org/10.1103/PhysRevLett.99.074502)

PACS numbers: 47.20.Ft, 47.27.Cn, 47.27.nf

Wall-bounded shear flows are of tremendous practical importance, yet their transition to turbulence is still poorly understood. The oldest and most famous example is the stability of flow along a straight pipe of circular cross section first studied over 120 yr ago [1]. A steady, unidirectional, laminar solution always exists, but is only realized experimentally for lower flow rates (measured by the Reynolds number $Re := UD/\nu$, where U is the mean axial flow speed, D is the pipe diameter, and ν is the fluid’s kinematic viscosity). At higher Re , the fluid selects a state which is immediately spatially and temporally complex rather than adopting a sequence of intermediate states of gradually decreasing symmetry. The exact transition Reynolds number Re_t depends sensitively on the shape and amplitude of the disturbance present and therefore varies across experiments with quoted values typically ranging from 2300 down to a more recent estimate of 1750 [2]. A new direction in understanding such abrupt transition in this and other wall-bounded shear flows revolves around identifying alternative solutions (beyond the laminar state) to the governing Navier-Stokes equations. So far, a universal structure has emerged for these solutions consisting of wavy streaks with staggered quasistreamwise vortices as found recently in channel [3–6] and pipe flows [7,8]. In the latter, these solutions take the form of unstable traveling waves (TWs)—saddle points in phase space—which appear through saddle node bifurcations. The lowest bifurcation is found at $Re_g = 1251$, which provides an upper estimate of when the laminar state stops being a global attractor. The delay before transition occurs ($Re_t \geq 1750$) is attributed to the need for phase space to become sufficiently complicated (through the entanglement of stable and unstable manifolds of an increasing number of saddle points) to support turbulent trajectories.

In this Letter, we significantly lower the threshold Reynolds number Re_g for these alternate solutions to appear from 1251 to 773 by uncovering a new family of “mirror-symmetric” traveling waves. Not only do these

waves preempt existing TWs [7,8], but they appear more dynamically important given the extremes of their wall shear stress. They also suffer a symmetry-breaking bifurcation to spawn particularly striking “asymmetric” modes, which represent what looks to be a minimal coherent unit: one slow streak sandwiched between two fast streaks located preferentially to one side of the pipe. Both the mirror-symmetric and asymmetric modes have no discrete rotational symmetry about the pipe axis in contrast to existing TWs. The fact that the ratio of Re_g to Re_t in pipe flow is now comparable to that for plane Couette flow ($Re_g = 127.7$ [3,6] and $Re_t \approx 320$ [9]) suggests that the mirror-symmetric TWs are close to if not the first family of alternative solutions to appear as Re increases. Helical and nonhelical rotating waves are also presented to emphasize the richness of phase space at these low Reynolds numbers.

The new solutions were captured by inserting a fully three-dimensional spectral representation [Chebyshev in s , Fourier in ϕ and z , where (s, ϕ, z) are the usual cylindrical coordinates aligned with the pipe] of the velocity and pressure field into the governing Navier-Stokes equations as viewed from an appropriately rotating and translating reference frame in which the TW is steady [8]. The resultant nonlinear algebraic system was solved using the Newton-Raphson algorithm [10]. To start the procedure off, an artificial body force was added to the Navier-Stokes equations (see [8]) designed to give streamwise-independent vortices and streaks of a finite amplitude. The size of the forcing was then adjusted to find a bifurcation point at which the translational flow symmetry along the pipe is broken. New finite-amplitude solutions to pipe flow were found if this solution branch could be continued back to the zero-forcing limit.

The TWs previously isolated [7,8] were induced using a forcing that was rotationally symmetric under

$$\mathbf{R}_m: (u, v, w, p)(s, \phi, z) \rightarrow (u, v, w, p)(s, \phi + 2\pi/m, z)$$

for some $m = 2, 3, 4, 5$, or 6. As well as this rotational symmetry, all the TWs also possess the shift-and-reflect symmetry

$$\mathbf{S}: (u, v, w, p)(s, \phi, z) \rightarrow (u, -v, w, p)(s, -\phi, z + \pi/\alpha),$$

where α is the base axial wave number (so the periodic pipe is $2\pi/\alpha$ long), and take the form $\mathbf{u}(s, \phi, z, t) = \mathbf{u}(s, \phi, z - Ct)$, where C is the *a priori* unknown axial phase speed of the wave. In contrast, new rotationally asymmetric TWs were found by using a forcing function which created vortices with the radial velocity structure $u(s, \phi) \propto \Re\{e^{-1/s}(1 - s^2) \sum_{m=1}^7 [1 + \cos(\frac{m\pi}{7})] e^{im\phi}\}$ and hence distributed energy across a band of azimuthal wave numbers. This choice led to a branch of asymmetric solutions whose component fast and slow streaks are preferentially located to one side of the pipe (see Fig. 1) just like the asymmetric wave discovered in channel flow [11]. These asymmetric TWs are \mathbf{S} symmetric and have one phase speed C along the pipe. For the wave number $\alpha = 0.75$, they extend beyond $\text{Re} = 5000$ and reach down to

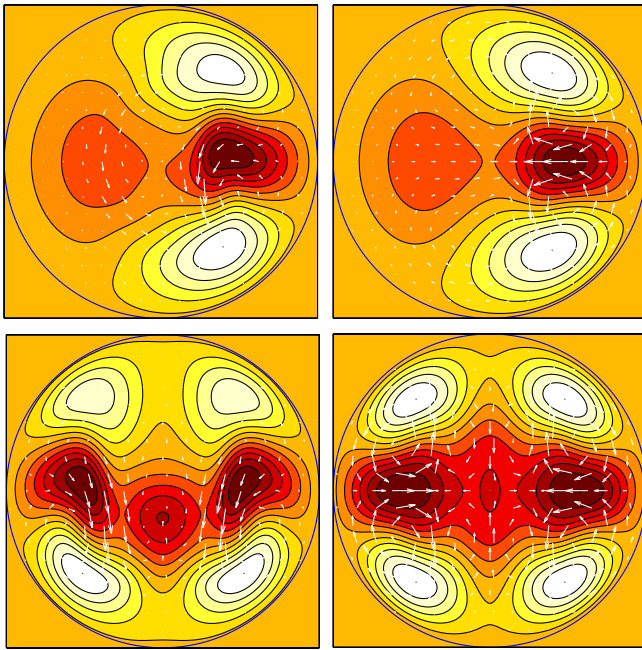


FIG. 1 (color online). Velocity fields for the asymmetric mode at $\text{Re} = 2900$ (top) and the mirror-symmetric mode at $\text{Re} = 1344$ (bottom) (both at $\alpha = 0.75$). An instantaneous state is shown on the left and a streamwise-averaged state on the right. The coloring indicates the downstream velocity relative to the parabolic laminar profile: red (dark) through white (light) represents slow through fast (with zero corresponding to the shading outside the pipe). In-plane velocity components are shown by vectors. The maximum and minimum streamwise velocities (with the laminar flow subtracted) and maximum in-plane speed for the asymmetric mode are 0.33, -0.42 , and 0.03, respectively, while for the mirror-symmetric mode they are 0.31, -0.43 , and 0.08 (all in units of U).

$\text{Re} = 1770$, where they arise in a supercritical pitchfork bifurcation from a mirror-symmetric TW family (see Fig. 1), which satisfies the additional shift-and-rotate symmetry

$$\mathbf{\Omega}: (u, v, w, p)(s, \phi, z) \rightarrow (u, v, w, p)(s, \phi + \pi, z + \pi/\alpha)$$

(coupled with the \mathbf{S} symmetry, this implies invariance under reflection in the line $\phi = \pm\pi/2$). The mirror-symmetric solutions, which also have known channel analogues [4–6], undergo a saddle node bifurcation at much lower Re : $\text{Re} = 1167$ at $\alpha = 0.75$, going down to a minimum of $\text{Re} = 773$ at $\alpha = 1.44$; see Fig. 2. At $\alpha = 1.44$ the pitchfork bifurcation which gives rise to the asymmetric modes is now subcritical with a saddle node bifurcation at slightly lower Re .

Both new families possess the universal features of such solutions in wall-bounded shear flows: wavy streaks with staggered quasistreamwise vortices [3–8]. In a pipe, the fast streaks near the wall are essentially two-dimensional aligned with the flow direction, whereas the slow streaks in the interior have much more streamwise undulation. By continuity, however, helical TWs should exist with these fast streaks inclined to the flow direction, and indeed a surface of such solutions can be found connecting the upper and lower branches of the mirror-symmetric TWs (see Fig. 3). These helical TWs take the form $\mathbf{u}(s, \phi, z, t) = \mathbf{u}[s, \phi - \beta(z - Ct) - \omega t, z - Ct]$ with β measuring the helicity in the Galilean frame moving at $C\hat{z}$ and ω being an azimuthal phase speed *relative* to the Galilean frame. Helicity destroys \mathbf{S} symmetry, but a modified form of $\mathbf{\Omega}$ symmetry ($\mathbf{\Omega}_\beta$) is preserved where the rotation transformation is now $\phi \rightarrow \phi + (1 - \frac{\beta}{\alpha})\pi$. The helicity β and rotational speed ω never rise above

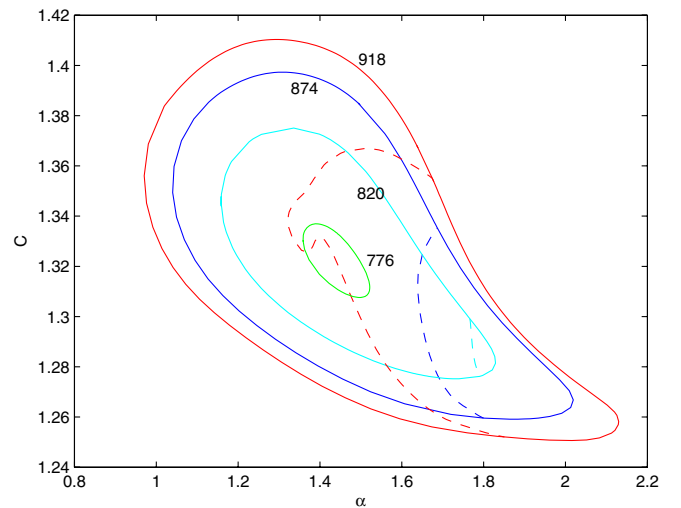


FIG. 2 (color online). Phase velocity C in units of U as a function of α for the mirror-symmetric modes (solid lines) and asymmetric modes (dashed) at 4 values of Re near the saddle node bifurcation at $\text{Re} = 773$.

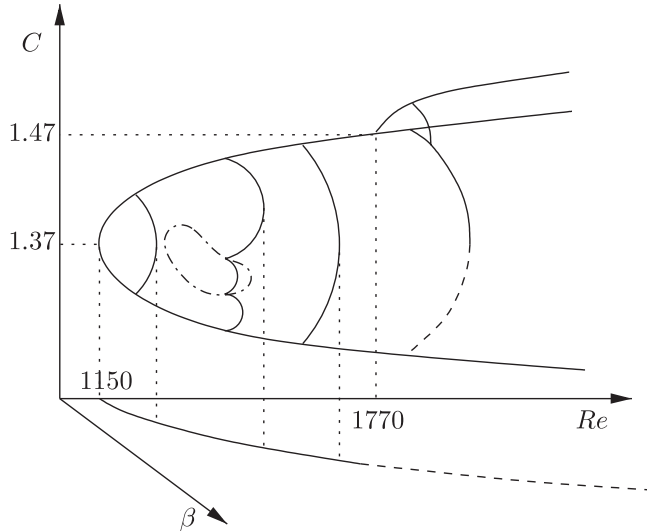


FIG. 3. A schematic picture of how all the new traveling wave branches fit together in (β, Re, C) space (at $\alpha = 0.75$). The main parabolic curve in the $\beta = 0$ plane is the mirror-symmetric branch off which the asymmetric branch bifurcates (uppermost line). Helical branches bulge out of the $\beta = 0$ plane and connect upper and lower parts of the mirror symmetric. Across a finite range of Re , these helical modes perforate the $\beta = 0$ plane in between the mirror-symmetric branches, creating an isola of nonhelical rotating TWs (closed dashed-dotted loop). Helical waves also connect the asymmetric branch and the helical solutions which originate from the mirror-symmetric solutions. [solid (dashed) lines indicate confirmed (inferred) behavior].

$O(10^{-2})$ for $Re \leq 1500$, confirming the flow preference for nonrotating, axially aligned streaks. Interestingly, in the range $Re = 1165$ – 1330 , the helicity β on this surface passes through zero twice in going between the two mirror-symmetric branches (see Fig. 3). These points correspond to an isola in the (fixed α) C vs Re plane of rotating nonhelical modes, which are neither shift-and-reflect symmetric nor have any rotational symmetry. The helical and nonhelical rotating waves look very similar to the mirror-symmetric modes except for a slight twist in the streak structure along the pipe (see Figs. 4 and 5). Helical modes continued off the asymmetric modes have no symmetry at all and originate in a symmetry-breaking bifurcation off the Ω_β -symmetric helical solutions extended from the mirror-symmetric waves: see Fig. 3.

The wall shear stress associated with a TW is a suggestive measure of how “far” the TW is from the laminar state in phase space, correlating strongly with the numerical truncation needed for its representation. Figure 6 shows a nondimensionalized measure of this—the friction factor $\Lambda := 2DG/\rho U^2$ (where G is the mean pressure gradient along the pipe and ρ the density)—as a function of Re for all the TWs. The new rotationally asymmetric waves clearly attain the lowest and the highest wall shear stress and by implication exist “nearest” and “further” from the laminar state. The former observation is particularly sig-

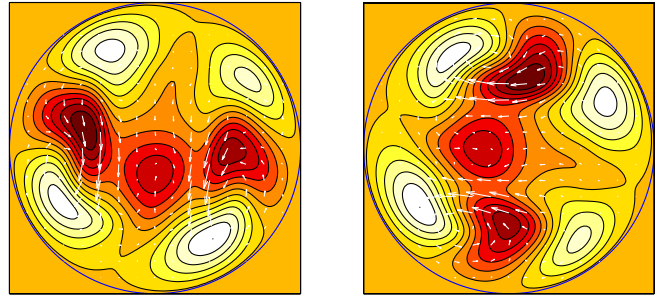


FIG. 4 (color online). Two velocity slices across a helical mode taken at the same instant of time but $25D$ apart with $\alpha = 0.75$, $\beta = 0.019$, $\omega = -0.0011$ at $Re = 1344$. The velocity representation is as in Fig. 1.

nificant since low-friction-factor (lower branch) TWs appear to sit on a dividing surface in phase space (a separatrix if the turbulence is a sustained state), which separates initial conditions which directly relaminarize and those which lead to a turbulent episode. Numerical simulations have confirmed this for 4 TWs in pipe flow [12], and for 1 TW in both plane Poiseuille [11] and plane Couette flow [13]. The new mirror-symmetric and asymmetric TWs [14] now give points where this dividing surface comes closer to the laminar state than before and through their stable manifolds plausibly give the closest point of approach. This point in phase space gives both the threshold amplitude and optimal structure for a disturbance to the laminar state not to decay, an issue of considerable current interest [15–18]. Interestingly, computations using a shooting technique to converge onto this dividing surface [17] have found an aperiodic state which, when temporally averaged, bears a remarkable similarity to the asymmetric TW found here (compare Fig. 1 at $Re = 2900$ to Fig. 5 of [17] at $Re = 2875$). This implies that more complicated states which originate through a bifurcation sequence from a TW can also populate this dividing surface.

The significance of the high friction factors associated with the upper branch of the mirror-symmetric TWs is their possible connection with the turbulent state itself. While there is mounting experimental [19,20] and numerical evidence [12,21] which indicates that TWs appear as transient but recurrent coherent structures within transitional flows, these are not immediately the TWs with highest friction factors. However, as Re increases, the part of phase space populated by the turbulent flow appears to expand to encompass more and more of the high wall shear stress states, which then assume increasing dynamical importance [12,22].

The friction factors associated with the helical modes interpolate between those of the corresponding nonhelical upper and lower branches. The inset to Fig. 6 shows how the phase speeds of the new rotationally asymmetric waves slot naturally into the spectrum of speeds shown by the rotationally symmetric waves.



FIG. 5 (color online). The four fast streaks of the helical mode shown in Fig. 4 plotted over one β wavelength $\approx 170D$.

The asymmetric, mirror-symmetric, and helical TWs all represent saddle points in phase space with very low-dimensional unstable manifolds [e.g., 2 for the asymmetric mode at $(\alpha, Re) = (0.75, 1820)$ and 4 for the mirror-symmetric mode at $(\alpha, Re) = (0.75, 1184)$]. Their presence indicates the richness of phase space even at Reynolds numbers approaching 773. Pipe experiments including neutrally buoyant particles [23] can show turbulence at $Re \approx 1000$, but for Newtonian fluids, the delay of transition until $Re \geq 1750$ suggests that the establishment of a “turbulence-bearing” scaffold constituted of all their stable and unstable manifolds is far from immediate. The clear conclusion is that while the emergence of alternative solutions to the laminar state seems a necessary precursor

for transition, it is *not* a good predictor of the actual Reynolds number at which this occurs in pipe flow (and other shear flow systems).

We acknowledge encouraging discussions with Fabian Waleffe and the support of EPSRC.

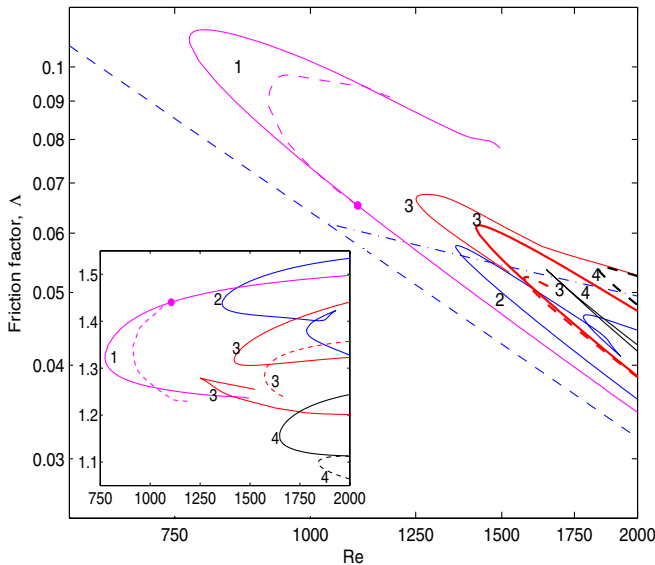


FIG. 6 (color online). Friction factor Λ against Re for the various TW families. The lower dashed line indicates the laminar value $\Lambda_{\text{lam}} = 64/Re$ and the upper dash-dotted line indicates the log-law parametrization of experimental data $1/\sqrt{\Lambda} = 2.0 \log(Re\sqrt{\Lambda})$. The labels are m values for the rotational symmetry \mathbf{R}_m of the different TW families all drawn at the wave number which leads to the lowest saddle node bifurcation. The new TWs shown—mirror-symmetric modes (solid) and asymmetric modes (dashed)—correspond to $m = 1$ and $\alpha = 1.44$. The bifurcation point where the asymmetric waves are born is marked with a dot. The inset shows the phase velocity C (in units of U) versus Re for all the TWs (upper branch TWs have smaller phase speeds than lower branch TWs).

*Chris.Pringle@bris.ac.uk

†R.R.Kerswell@bris.ac.uk

- [1] O. Reynolds, Proc. R. Soc. London **35**, 84 (1883).
- [2] J. Peixinho and T. Mullin, Phys. Rev. Lett. **96**, 094501 (2006).
- [3] M. Nagata, J. Fluid Mech. **217**, 519 (1990).
- [4] F. Waleffe, Phys. Rev. Lett. **81**, 4140 (1998).
- [5] F. Waleffe, J. Fluid Mech. **435**, 93 (2001).
- [6] F. Waleffe, Phys. Fluids **15**, 1517 (2003).
- [7] H. Faisst and B. Eckhardt, Phys. Rev. Lett. **91**, 224502 (2003).
- [8] H. Wedin and R. R. Kerswell, J. Fluid Mech. **508**, 333 (2004).
- [9] S. Bottin, O. Dauchot, F. Daviaud, and P. Manneville, Phys. Fluids **10**, 2597 (1998).
- [10] In the nomenclature of [8], typical resolutions used to represent the modes were (15, 25, 5), representing about 20 000 degrees of freedom.
- [11] T. Itano and S. Toh, J. Phys. Soc. Jpn. **70**, 703 (2001).
- [12] R. R. Kerswell and O. R. Tutty, J. Fluid Mech. **584**, 69 (2007).
- [13] J. Wang, F. Gibson, and F. Waleffe, Phys. Rev. Lett. **98**, 204501 (2007).
- [14] At $\alpha = 0.75$ the asymmetric TW branch bifurcates supercritically off the lower mirror-symmetric TW branch and actually has a slightly lower friction factor.
- [15] B. Hof, A. Juel, and T. Mullin, Phys. Rev. Lett. **91**, 244502 (2003).
- [16] F. Mellibovsky and A. Meseguer, Phys. Fluids **18**, 074104 (2006).
- [17] T. M. Schneider, B. Eckhardt, and J. A. Yorke, arXiv:org/nlin/0703067.
- [18] J. Peixinho and T. Mullin, J. Fluid Mech. **582**, 169 (2007).
- [19] B. Hof *et al.*, Science **305**, 1594 (2004).
- [20] B. Hof, C. W. H. van Doorne, J. Westerweel, and F. T. M. Nieuwstadt, Phys. Rev. Lett. **95**, 214502 (2005).
- [21] T. M. Schneider, B. Eckhardt, and J. Vollmer, Phys. Rev. E **75**, 066313 (2007).
- [22] A. P. Willis and R. R. Kerswell, arXiv:org/abs/0706.3330.
- [23] J.-P. Matas, J. Morris, and E. Guazzelli, Phys. Rev. Lett. **90**, 014501 (2003).